ELECTRON MULTIPLIER INVESTIGATIONS

THESIS FOR THE DEGREE OF ELECTRICAL ENGINEER

WARREN HERBERT BLISS

1939

ELECTRON MULTIPLIER INVESTIGATIONS

A Thesis Submitted To

The Graduate Council of

Michigan State College

of

Agriculture and Applied Science

by

Warren Herbert Bliss

Candidate for the Degree

of

Electrical Engineer

June, 1939.

THESIS

Electron Multiplier Investigations

Table of Contents

121475

References

1. The Secondary Emission Multiplier - A New Electron Device. V. K. Zworykin, G. A. Morton, and L. Malter. March 1936. Issue of Proceedings of the Institute of Radio Engineers.

2. Secondary Emission Electron Multiplier. An article in the November, 1935 Issue of Electronics.

3. Electrostatic Focussing in Secondary Emission Multipliers. Engineering Report TR-362, RCA Victor Division, by J. Rajchman and E. W. Pike.

1 - Synopsis

1.1 - Purpose of the Investigation

The investigation which is outlined in this report was carried out with the following threefold object as a guide:

(A) To obtain a working knowledge of light controlled, secondary emission, electron multiplier tubes.

(B) To determine the practicability of vacuum tubes of this type when employed with suitable circuits and auxiliary equipment to generate high speed facsimile test waveforms.

(C) To consider a few possible scanner arrangements and briefly outline for reduction to practice those that are found to be suitable.

1.2 - General Procedure

A ten stage, photoelectric type, secondary emission electron multiplier tube was obtained from the Radiotron Division at Harrison and a test "tea-wagon" was built up to house the equipment which included a television receiver type power pack obtained from the Victor Division at Camden and a 1500 volt rectifier. A special light source, lens system, and chopper disc assembly was constructed for supplying light to the tube.

Static and dynamic characteristics were determined, the latter tests being made principally at 60 and 12,000 cycles per second.

A few tests were made to determine the feasibility of introducing an a-c carrier frequency into the electron multiplier so that a light modulated a-c wave would result in the output. This was tried electrostatically and magnetically.

The electron multiplier output was also used in a balanced modulator to modulate a 75 kc carrier. In connection with this a special compensating or counter emf circuit was used to improve the linearity of the modulator. The re-occurring phenomena generated by the specially prepared chopper disc was used successfully to test facsimile terminal facilities at keying speeds up to 12,000 cycles per second.

1.3 - General Statement of Findings

On the basis of information obtained to date the electron multiplier has a very definite promise of providing at least one scheme for satisfactorily scanning subject matter at "page a minute" speed. The apparatus arrangement to be described provides an extremely flexible tool for use in the investigation of high speed facsimile terminal and radio circuit requirements.

2. Recommendations

Experience with the electron multiplier test assembly described in this report indicates that it can be successfully employed to generate accurately controlled high speed facsimile test phenomena. It is accordingly recommended for studying terminal and radio circuit requirements.

It is also recommended that the study of the general performance characteristics of various electron multiplier modifications be continued in cooperation with the Victor and Radiotron divisions of RCA-Manufacturing.

Also, as time permits, that detailed consideration be given the following:

(a) Introduction of carrier ac into the multiplier by the electrostatic method.

(b) Determination of the minimum number of multiplier stages or minimum total voltage necessary to give sufficient output for scanner applications.

(c) Further development of a suitable modulator, probably a balanced type.

(d) If theoretical considerations and preliminary experimental work indicate the desirability, the construction of a high speed scanner using a suitable electron multiplier tube as a pick-up unit.

3. Detailed Discussion of Investigation

3.1 - Statement of Problem

For the study of terminal and radio circuit requirements for the successful handling and transmission of high speed facsimile signals it was desirable to have a test apparatus or device which would produce such signals or waveforms of voltage and current. Ordinary vacuum tube oscillators do not readily produce these and high speed scanners were still in the process of development.

Furthermore, there was still the desirability of determining a suitable scanner to be used in a facsimile system capable of handling a letter size sheet per minute. In present speeds of facsimile operation there is barely enough output from the photocell to operate circuits of minimum acceptability. Higher speed operation requires improved response, especially a linear frequency characteristic covering a wider band. Higher outputs are also desirable, since, with these, some of the well known types of modulators could be controlled directly.

The photoelectric type, secondary emission electron multiplier appeared to be a unit which would supply both of the needs outlined above. Hence, it was decided to make a preliminary investigation of the characteristics and some possible applications of multipliers.

3.2 - Resume of Electron Multiplier Theory

The construction, theory and operation of secondary emission multipliers has been described at length in Reference 1. A brief treatment will be given here to familiarize the reader with the functioning of the magnetic, photoelectric type.

Fig. 1 of Sheet A shows the arrangement of electrodes and resistors inside the tube and also the usual external connections for a 10 stage experimental tube.

The electrodes are divided into two general groups ------ accelerating plates and emitters. Electrodes b, d, f, h, j, l, n, p, r and t belong to the former group and a, c, e, g, i, k, m, o, q and s to the latter. v is the collector and u, the screen. In the tube used in this investigation the first 6 accelerating electrodes were made of screen so that light could be focused on any one of the first 6 emitters.

The multiplying action in the tube is a result of the ratio of secondary emission electrons to bombarding electrons on the emitters being greater than unity. Light, falling on the first emitter a, releases electrons by photoemission (the emitters are capable of photoelectric emission as well as secondary emission). These electrons are attracted by and accelerated toward electrode b which is at a higher potential than a. Except for the presence of a magnetic field whose lines of force are at right angles to the plane of the sketch in Fig. 1, sheet A, the electrons would go to plate b. However, the combined influence of the electrostatic and magnetic fields causes the electron path to be curved as shown in the sketch so that the electrons arrive at plate c which is at the same potential as b. The electron velocity at this bombarding point is sufficient to cause appreciable secondary emission.

A ratio of secondary electrons to primary electrons of 3 per stage can readily be obtained in a 10 stage multiplier. The increased number of electrons emitted by plate c is acted on by the next accelerating electrode and the magnetic field and then bombards plate e. In this manner the electron streams are amplified as they pass down the tube until the last plate v collects the final emission from s.

The distribution of voltage on the numerous electrodes is accomplished by means of a tapped resistance bleeder. To avoid having too many terminals on the tube the bleeder resistors for the first few stages are mounted inside the tube envelope. The output current may be passed through a resistor R_L where an emf proportional to the light will be developed.

3.3 - <u>The Physical Setup</u>

3.31 - <u>General</u>

Fig. 1 of Photograph R-319 shows the general arrangement of the electron multiplier test setup. This shows the top compartment of the "tea-wagon" with the light source and chopper disc assembly. This compartment is 26 inches wide by 17 inches deep by 15 inches high. The front and top, which are on hinges so they may be turned up and back out of the way, are equipped with interlocking switches so that the power supplies (1500 volts and 6300 volts) cannot be turned on while the compartment is open. The top, front and right hand end are made of transparent material so that meters may be observed from outside. The bleeder or voltage divider resistor bank is mounted in the back of the compartment and the output meter and inner tube compartment, toward the front.

Fig. 2 of Photograph R-320 is an inside view of the inner tube compartment taken from above. The field magnet is shown pulled back to bring the tube into view. A rotatable base is controlled by an external knob so that the tube may be turned about its axis to bring it into proper relation with the magnetic field. Slots through both compartments provide an unobstructed path for the light beam.

Photograph R-344 and Fig. 1 of Photograph R-320 show the light source assembly. This unit was made to simulate the reflected light produced in an actual scanner. It was designed to comply with this in three respects:

1st, same aperture distortion, 2nd, same light quantity, and 3rd, same top frequency of light fluctuation for page a minute speed. The assembly consists of a lamp house, 10 volt lamp, a lens barrel, and a motor driven chopper disc.

3.32 - Details of Light Source Assembly.

Fig. 2 of Sheet A gives the details of the optical system. The light is supplied by a 50 watt, 10 volt lamp 1 which is operated at 8.5 volts. The first unit in the lens barrel is a condenser lens 2. From this the light passes through two screens 3 and 4. The first is one of fixed density which was chosen so that the light output of the system falling on plate 11 would be the same as that reflected from a conventional scanner drum for white subject matter. This value is about 6.4×10^{-4} lumen. Screen 4 is a stepped, density wedge slide, the top of which may be seen in Photograph R-344 projecting upward to the right of the lamp house.

The next important part of the optical system is the aperture 5. Two of these were used; the first one was 0.025 inches square and the second, 0.012 inches high by 0.025 inches long. These values, as will be explained later gave the desired aperture distortion.

Lens 6 focuses the image of aperture 5 on the chopper disc 8. A mask 7, having a small round hole through its center, cuts out most of the stray light arriving at this section. Lens 10 picks up the light as it comes through the chopper disc and brings it to a 5 millimeter spot on the photoelectric cathode 11 of the tube which is to receive the light.

A close inspection of Fig. 1, Photograph R-320 reveals the details of the chopper disc which is driven at 1800 RPM by a 60 cycle, synchronous motor. Two alternate 90 degree segments of the disc are solid. The other two alternate 90 degree segments are divided radially into six different bands. The outer or first band is cut away so that when this position is used 60 cycles per second square wave chopping is done. The second band has 100 teeth and 100 slots, each 0.032 inches wide, in each of the two 90 degree segments. This band, then, produces 12,000 cycles per second chopping. The next four bands produce, respectively, 4 impulses, 3 impulses, 2 impulses, and 1 impulse of 12,000 cycles. The disc drive motor is mounted on a sliding base so that any one of the six bands may be brought into the light beam at the proper point.

3.33 - Chopper Frequency Considerations and Aperture Distortion

For a 10 inch page per minute scanning the

$$\text{Screw Advance} = \frac{10}{60} = 0.1667 \text{ inches/sec.}$$

For standard line advance of 120 lines per inch the

Screw Advance = 0.1667 x 120 = 20 lines/sec.

For a standard drum circumference of 9.22 inches the

Linear Scanning Speed = 20 x 9.22 = 184.4 inches/sec.

The stems and bars of letters of 8 point type are 0.0082 inches wide. Taking twice this value or 0.0164 inches as the length of a cycle in scanning such letters, the following is obtained.

Maximum Fundamental Scanning Frequency for Page a Minute Speed

= 184.4/0.0164 = 11,244 cycles/second.

Hence, the chopper disc was designed to simulate 12,000 cycle scanning, which is a slightly greater requirement than that actually expected.

In the standard AA-914 Scanner the light spot as it strikes the drum surface is 0.006 inches by 0.008 inches. The first dimension is that measured parallel to the direction of motion of the drum surface at the scanning point. Hence, the period of aperture distortion in scanning a letter bar cycle (= 0.0164 inches) is given as

$$\text{Aperture distortion} = \frac{0.006}{0.0164} = 0.366 \text{ cycle}$$

$$= 0.366 \times \frac{1}{11{,}244} = 32.5 \times 10^{-6} \text{ sec.}$$

$$= 32.5 \text{ microseconds}$$

for page a minute scanning.

In designing the chopper disc a diameter of 8 inches was selected. Too large a disc would require a large motor and too small a disc would require teeth and slots too small to be made accurately. With the 8 inch disc the teeth were made with a 1/32 inch cutter and spaced about 1/16 inch apart (center to center). This made the finished teeth and slots each practically 0.032 inches wide.

For the same aperture distortion as discussed above the light spot should have a

$$\text{Width} = 0.366 \times \frac{1}{16} = 0.0228 \text{ inch}$$

The aperture 5 (Fig. 2, sheet A) was actually made 0.025 inches square which gave slightly more distortion.

The oscillograms shown on Photograph sheet R-332 were made with this aperture. Since the duration of the flat top of the wave was very short another aperture having a width of 0.012 inch was made. The oscillographic results of this are shown on Photograph sheet R-333.

3.4 - <u>Static Characteristics</u>

Figs. 1 and 2 on sheet B are sketches of the circuits used in determining some of the static characteristics of the electron multiplier and on sheets C and D are the curves resulting from these tests.

The double, heavy voltage divider system shown in the circuit diagrams was used to insure good voltage regulation at all the multiplier terminals. Practically all the tests were made with a total potential of 1500 volts which was divided into 130 volts per stage and 200 volts for the collector or anode. With this condition and zero resistance in the anode circuit the data for the resonance and linearity characteristics shown on sheet C were taken.

Fig. 1 shows the relationship between the anode current and the magnetic field strength for the major resonance peak. This curve is similar to one shown in reference 1 and shows the necessity of holding the field coil current constant. It was observed that operation of the tube on either side of the resonance peak caused appreciable noise in the output resulting from small irregularities in the high voltage or field supplies. The most stable operation, as well as the maximum output, was obtained when the conditions were such that the tube was performing at the top of the resonance hump. The amount of light used in this test was about 5×10^{-4} lumen.

Fig. 2 of sheet C is a linearity check on the multiplier for small quantities of light. A light density wedge was calibrated by means of a standard type 918 photocell with a comparatively large amount of light and then the wedge was used to check the multiplier with about 5×10^{-5} lumen maximum. No data was taken for large amounts of light since the saturation point was believed to be well above one milliampere of output current.

Figs. 1 and 2 on sheets B and D show the test circuits and results of variation of load resistance. Fig. 1 on each sheet is the case for normal operation with the load resistor in the anode circuit. With this condition the output terminal at ground potential is the plus lead. The circuit was also arranged as in Fig. 2, sheet B, so that output voltage of reversed polarity with respect to ground could be obtained. In this case the terminal at ground potential is the negative lead. Both of these schemes were tried because either polarity, with respect to ground, may be desirable depending on the type of modulation to be produced. It should be noted that there may be objections to the second scheme since the variation in IR drop across the load resistor alters the potential of the last emitter and the accelerating electrode connected to it. However, the curves for output voltage are similar in shape, and in practice the load resistance may be kept low enough to limit the output to a few volts so that this alteration of electrode potentials may not be objectionable.

The two tests discussed above were conducted with 6.4×10^{-4} lumen of light, which value, as mentioned previously, is equivalent to that reflected from white subject matter on a standard facsimile drum. This value was determined by measuring the current in a type 918 phototube when receiving the reflected scanner light. The light from the light chopper lens system was then directed into the same cell and a light screen selected to produce the same cell current. It was assumed that discrepancies due to color differences in the two sources could be neglected. The numerical value given above results from the rated sensitivity of a 918 cell (110 microamp./lumen) and the measured cell current (0.07 microamps.)

3.5 - Dynamic Characteristics (Experimental)

Photographs R-332 and R-333 are the results of a series of tests on the electron multiplier when operating with "chopped" light. The circuit of Fig. 1, sheet B, was used to obtain all of these. For the oscillograms on R-332 the aperture distortion was 32 microseconds for the 60 and 12,000 cycle tracings and 48 microseconds for the 8000 cycles while the quantity of light for all was about 10^{-3} lumen. For those on R-333 the aperture distortion was 16 microseconds and the quantity of light, 6.4×10^{-4} lumen. These two groups of oscillograms were obtained by contact exposure prints on the glass screen of the RCA type TMV-122-D oscillloscope, whose vertical sensitivity was 90 volts per inch.

In considering sheet R-332 the effect of load resistance and capacitance on the wave form is not very evident except for the 60 cycle square waves. The influence of these factors on magnitude is quite prominent, however. Referring to Figs. 1 and 5 or to Figs. 2 and 6, the output voltage is seen to be proportional to the load resistance as would be expected. In Fig. 5 the output voltage peaks are 70 volts. A comparison of Figs. 2 and 4 shows a decrease in magnitude due to the current shunting effect of a small condenser in parallel with the load resistance. The aperture distortion was so great for these cases that the waves appear to be almost sinusoidal.

The 8000 cycle oscillograms were obtained by driving the chopper motor from a 40 cycle mechanical fork supply. The tendency for flat top on the waves is evident in Fig. 1. The theoretical duration of flat top in this case is 1/8 of a cycle. In spite of the efforts to reduce the stray capacitance to an absolute minimum the corners of the waves are still slightly rounded.

Fig. 7 shows the quality of wave form for 60 cycle square wave with an aperture distortion of 32 microseconds. This wave is perfect for most practical purposes. Fig. 8 shows that the shunt or stray capacitance can be as great as 0.005 mfd. before this waveform is altered appreciably.

The waveforms on sheet R-333 give a better indication of the dynamic performance of the multiplier. With the aperture distortion reduced to 16 microseconds the flat-topped nature of the waves is very pronounced. Figs. 9, 11 and 13 show the effect of varying the load resistance; With values of 100,000 ohms or higher the flat top is distorted. For a 50,000 ohm load the waveform is good and the peak value of voltage is 22 volts; this is from 6.4×10^{-4} lumen of light. Reducing the load resistance below 50,000 ohms improves the wave shape slightly but decreases the output voltage directly.

Figs. 10, 12 and 14 show the influence of shunt capacitance. The first and last of these were taken with a load circuit time constant of 10 microseconds which distorts the waveshape appreciably. The wave of Fig. 12, which was made with a time constant of 5 microseconds, might be regarded as the limit of allowable distortion but even in this case there is a time lag which does not show up in the oscillogram. See section 3.6 of this report for explanation of this lag.

Figs. 9 and 15 were made with identical circuit conditions but the latter was produced with the light quantity reduced considerably. This test was carried out to show that the waveform (except for change in magnitude) depends solely on the circuit constants. A close examination of these oscillograms will show that this is true. The magnitudes are different but the forms are the same.

Fig. 16 was made to show the effect of light saturation on the output waveform. The peak value of current in this case was about 5 milliamperes and the light, several times normal.

3.6 - Dynamic Characteristics (Theoretical)

The response of the load circuit of the multiplier to the output current wave caused by incident light fluctuation can readily be determined mathematically as follows:

Except for the case where the load circuit contains series inductance the output current from an electron multiplier or a photocell can be expected to follow the incident light fluctuation almost precisely. This is true only as long as these devices have sufficient anode potential to be well above the saturation point. The output current is then independent of the applied voltage.

It is the purpose of this treatment to show how much the voltage across the load resistance deviates from following the incident light variations when leakage or stray shunt capacitance exists across this load resistance. Two cases will be considered: First, the response to a single rectangular impulse, and second, the response to a single symmetrical trapezoidal impulse.

Case I

Fig. 1, sheet F, shows the circuit and notation that are to be used. For Case I i = f(t) will be defined by

$$\left.\begin{aligned} i &= f(t) = 0 && \text{for } t < 0, \\ i &= f(t) = I && \text{for } 0 < t < t_1, \\ \text{and } i &= f(t) = 0 && \text{for } t > t_1. \end{aligned}\right\} \qquad (1)$$

Applying Kirchhoff's First Law to the Circuit gives

$$i_C + i_R = i. \qquad (2)$$

Applying Kirchhoff's Second Law gives

$$R i_R = \frac{1}{C}\int i_C \, dt. \qquad (3)$$

Combining (2) and (3) produces

$$i = i_C + \frac{1}{RC}\int i_C \, dt. \qquad (4)$$

Heaviside's operational notation and method may readily be applied to (4).

$$\left(1+\frac{1}{PRC}\right) i_c = I\,1 \tag{5}$$

or $$i_c = \left(\frac{P}{P+\frac{1}{RC}}\right) I\,1 . \tag{6}$$

The solution of (6) is

$$i_c = I\,\epsilon^{-t/RC}. \tag{7}$$

Since the load voltage, e_L, is desired, it is obtained thus,

$$e_L = R\,i_R = R(I - i_c) = RI(1 - \epsilon^{-t/RC}). \tag{8}$$

This is a well recognized form. It is similar to the expression for the rise in current in an RL circuit when unit function voltage is applied. Fig. 1, sheet E, shows the rectangular impulse as plotted for the case of R = 50,000 ohms, C = 100 mmfd. and I = 5×10^{-4} amp., up to the point where $t = t_1$ = 30 microseconds.

Beyond where $t = t_1$ $i = o$ and $i_C = -i_R$. If the variable t is now measured from t_1 as a new zero point the condenser discharges through the resistor according to

$$i_R = I_R\,\epsilon^{-t/RC}, \tag{9}$$

where I_r is the initial value of the discharge current.

The load voltage in this case is

$$e_L = RI_R\,\epsilon^{-t/RC} \tag{10}$$

This has also been plotted on the same graph.

The complete curve shows the characteristic "rounding of the corner" effect that is frequently noticed when square wave is applied to amplifiers, filters and other circuits. The smaller the value of RC (the time constant), the more nearly the response approaches the actual applied waveform.

Case II

In facsimile scanning the light variation is never a true rectangular waveform due to aperture distortion. The theoretical

variation simulates a trapezoid as illustrated in Fig. 2 of sheet E. For this case i = f(t) may be defined by

$$\left.\begin{array}{ll} i=f(t)=0 & \text{for } t<0, \\ i=f(t)=Kt & \text{for } 0<t<t_1, \\ i=f(t)=I & \text{for } t_1<t<t_2, \\ i=f(t)=(Kt_2+I)-Kt & \text{for } t_2<t<t_3, \\ \text{and } i=f(t)=0 & \text{for } t>t_3. \end{array}\right\} \tag{11}$$

There are now four periods to consider.

Period A $(0<t<t_1)$

Equation (6) may be altered to apply in this case as follows:

$$i_c=\left(\frac{p}{p+\frac{1}{RC}}\right)Kt\,1, \tag{12}$$

since I now becomes Kt.

The solution of this equation can best be accomplished by application of the Superposition Theorem which is usually written in the following form taken from page 56 of "Operational Circuit Analysis" by Bush.

$$i_t=e(0)A(t)+\int_0^t A(t-\lambda)e'(\lambda)d\lambda. \tag{13}$$

In this, e(t) is usually the applied voltage function but will be Kt, the applied current, in our case. A(t) is the indicial admittance which, by equation (7), is $\epsilon^{-t/RC}$. We accordingly have the following values to substitute into equation (13):

$$\left.\begin{array}{l} e(0)=0 \\ A(t)=\epsilon^{-t/RC} \\ A(t-\lambda)=\epsilon^{-(t-\lambda)/RC} \\ e'(\lambda)=K \end{array}\right\} \tag{14}$$

Substitution of (14) in (13) gives

$$i_c = \int_0^t \epsilon^{-(t-\lambda)/RC} K d\lambda = K\epsilon^{-t/RC}\int_0^t \epsilon^{\lambda/RC} d\lambda. \qquad (15)$$

Integrating and simplifying (15) produces

$$i_c = KRC(1-\epsilon^{-t/RC}). \qquad (16)$$

The load voltage will accordingly be

$$e_L = Ri_R = R(Kt - i_c) = KRt - KR^2C(1-\epsilon^{-t/RC}) \qquad (17)$$

The curve resulting from this equation for period A is plotted in Figure 2 sheet E, for K = 31.2 amps./sec. and the other values as previously given.

An interesting and important fact is brought out by the above development and the resulting curve. The voltage rise across the load resistance lags behind the rise in light value and this lag quickly approaches a fixed value which can be determined as follows:

Let the voltage at time t_1 as given by equation (17) be V' (represented by point b on the curve). Hence

$$V' = KRt_1 - KR^2C(1-\epsilon^{-t_1/RC}). \qquad (18)$$

In the case of zero shunt capacitance the voltage V' would be reached in t_o seconds (point a) when

$$V' = KRt_o. \qquad (19)$$

Equating the right hand members of (18) and (19) and simplifying gives

$$t_1 - t_o = RC(1-\epsilon^{-t/RC}). \qquad (20)$$

As in the numerical example illustrated above, $\epsilon^{-t/RC}$ rapidly approaches zero as a limit as t is increased and (20) reduces to

$$t_1 - t_0 \doteq RC \qquad \text{for } t_1 >> RC. \tag{21}$$

The load voltage in practical cases soon lags the ideal wave by an amount equal to the time constant of the load circuit.

Period B $(t_1 < t < t_2)$

During this interval $i = f(t) = I$. Using i_r and i_c again as the current symbols and measuring time from $t = t_1$ as the new zero point, the application of Kirchhoff's laws gives

$$i_R + i_c = I \tag{22}$$

and $$R i_R = E_c + \frac{1}{C}\int i_c \, dt, \tag{23}$$

where E_c is the initial condenser voltage.

Solving (22) and (23) gives

$$i_c = I' \epsilon^{-t/RC}, \tag{24}$$

in which $$I' = \left(I - \frac{E_c}{R}\right).$$

From this

$$e_L = R i_R = R(I - i_c) = RI - RI'\epsilon^{-t/RC}. \tag{25}$$

This function is also plotted on the graph between the points marked t_1 and t_2. For the numerical values used e_L practically reaches the steady state value at the latter time, t_2.

Period C $(t_2 < t < t_3)$

Measuring t from t_2 as a new zero our fundamental equations become

$$i_R + i_c = I - Kt \tag{26}$$

and
$$R\,i_R = E_c + \frac{1}{C}\int i_c\,dt. \tag{27}$$

From these
$$i_c = \left(\frac{p}{p+\frac{1}{RC}}\right)\left[\left(I-\frac{E_c}{R}\right)-Kt\right]1. \tag{28}$$

Using the Superposition Theorem again gives
$$i_c = \left(I-\frac{E_c}{R}\right)\epsilon^{-t/RC} - K\int_0^t \epsilon^{-(t-\lambda)/RC}\,d\lambda \tag{29}$$

or
$$i_c = \left(I-\frac{E_c}{R}\right)\epsilon^{-t/RC} - KRC\left(1-\epsilon^{-t/RC}\right). \tag{30}$$

Then
$$e_L = RI + KR^2C - KRt + (E_c - RI - KR^2C)\epsilon^{-t/RC}. \tag{31}$$

The plot of this curve between t_2 and t_3 on the graph shows a lag on the voltage decay similar to that on the build-up. This, of course, is what was anticipated.

Period D $(t > t_3)$

Equation (10) will apply in this case
$$e_L = E_o\,\epsilon^{-t/RC} \tag{32}$$

t being measured from t_3 as a new zero and E_o is the value of e_L at t_3 from equation (31).

This completes the theoretical response curve of the load voltage.

Two facts have been brought out by the above considerations.

I. The original wave is changed in form by the presence of shunt capacitance.

II. The response for a trapezoidal wave lags the original wave by an amount which quickly approaches the time constant of the circuit as a limit.

The oscillograms of Photograph R-333 check the above theory in respect to the first fact but do not show the lag very well. A special test technique would be required for this. The same numerical values of the circuit factors were used to obtain the oscillogram of Fig. 12, sheet R-333, as were used for the theoretical case of Fig. 2, sheet E. The shape of these two curves is the same.

3.7 - Modulation Schemes

In facsimile systems for picture transmission via radio the light fluctuation picked up by the scanner is usually used to modulate an ac carrier. Several schemes were tried in connection with the electron multiplier as explained below.

3.71 - Carrier Applied Electrostatically to the Electron Multiplier

In order to determine the feasibility of introducing the carrier emf in series with one of the multiplier electrodes the static characteristic shown on sheet G was obtained by means of the circuit of Fig. 2, sheet F. The potential of number 3 electrode (this is actually the joint connection of emitter o and accelerating electrode n, see Fig. 1, sheet A) was varied over a wide range and the corresponding variation in load current noted. If the electrode is operated at a dc potential of + 40 volts with respect to the preceding electrode, a carrier emf having a peak value of 60 volts may be introduced. The output current should then vary directly with this carrier since the curve is linear over the range covered.

This scheme was tried with a 60 cycle square wave light variation and an 810 cycle carrier. Fig. 1 on Photograph R-334 is the resulting oscillogram of the output. This oscillogram was reproduced from a pencil tracing. The modulation envelope has two serious disadvantages. First, 100 percent modulation without distortion was impossible, and second the envelope has a variable dc component. There is no system known to the writer which will separate out the dc component of this type of wave without distorting the wave envelope. Unless this fundamental difficulty is overcome the electrostatic method of introducing the carrier does not appear promising.

3.72 - Carrier Applied Magnetically to the Electron Multiplier

An attempt was made to introduce the carrier by modulating the magnetic field of the multiplier. The results were less promising than for the electrostatic method. Not only did the modulation envelope contain the undesirable ac component but considerable power was necessary from the carrier supply in order to vary the magnetic field a sufficient amount.

3.73 - Use of a Push-Pull Modulator with the Electron Multiplier.

Because of the fundamental difficulties mentioned above (section 3.71) in trying to introduce the carrier into the multiplier itself the next logical scheme seemed to be to take the normal multiplier output and drive a suitable type modulator. A push-pull modulator using a double triode was set up so that the grids were excited 180° out of phase with the carrier and in phase (or in parallel) with the multiplier output.

A linearity check was made on the push-pull unit by varying the common bias voltage and noting the variation of ac output. The circuit of Fig. 1, sheet H, was used for this test and Fig. 1, sheet I, is the characteristic obtained. This curve shows a linear relationship over most of its range but is not linear for small values of output. This is important because a high ratio of output for white to black is desired in picture scanning.

Fig. 2, sheet H, shows a circuit whose modulation characteristic is linear down to zero. The fundamental idea of this system is that the carrier is balanced out of the output for the lower non-linear part of the normal characteristic. A counter emf circuit composed of transformer T_1, resistors R_1 and R_2, and condenser C supply a voltage of the proper phase and magnitude to balance out all the output represented by point A on Fig. 1, sheet I. Hence, point A on this curve becomes the virtual point of zero output. Fig. 2 is the actual modulation characteristic which results. This is linear down to the zero point and oscilloscope observations indicated that the waveform was also good over this range.

The next test was an overall linearity check of the electron multiplier and modulator combination. Fig. 1, sheet B, shows the multiplier circuit used, the output of which was applied to the modulator circuit of Fig. 2, sheet H, in series with lead A-B. Fig. 1, sheet J, shows the result. This curve has a negative slope because of the multiplier connection used which gave an output emf increasing in the negative direction as the light increased. The overall characteristic, which was made with a 5 kc carrier, is very good as indicated by the small deviation of points from the curve which was drawn with a straight edge. The amount of light used was about ten percent of that obtained in a standard photoradio scanner. (The latter was measured sometime after the linearity test had been made.)

The system described above was operated with 60 cycle square wave fluctuation of light and the results were good as observed on the oscilloscope except that difficulty was had in balancing the modulator to keep the dc transient "kick" of the multiplier output from appearing in the modulation envelope. This difficulty has now been overcome as will be mentioned later in this report.

3.74 - 75 KC Tests

In order to determine the performance of the electron multiplier with a modulator at frequencies in the general range of page-a-minute speed a "bread-board" setup of a 75 kc oscillator and modulator were made. This particular value of carrier frequency was chosen well above the minimum value necessary for page-a-minute speed in order that there would be several cycles of carrier per cycle of light fluctuation. Hence, the modulation envelope could be more accurately observed.

Fig. 2 of Photograph R-319 is a view of the 75 kc oscillator and modulator units and Fig. 1 of Sheet K is the combined circuit of the multiplier and modulator. In this case the latter unit gets its fixed bias voltage from the IR drop across part of one of the bleeder resistors in the multiplier circuit. Also the multiplier circuit is arranged to drive the modulator so that its ac output is directly proportional to the incident light instead of inversely as was the case of previous tests.

Fig. 2, Photograph R-334, shows a tracing of an oscillographic observation of the modulated 75 kc carrier. This was made with a 12 kc light fluctuation and an aperture distortion of 32 microseconds. A peak value of 10 volts across the 500 ohm load was easily obtained. This is good evidence that with additional development the multiplier would be suitable for high speed scanning.

One of the problems to be solved in this connection is that of finding a suitable balanced modulator. In all the tests so far described considerable difficulty was had, as mentioned previously, in balancing the modulating emf entirely out of the output. This problem was discussed with engineers of the Electronic Research Laboratory at Camden and they suggested using a push-pull modulator with tetrodes. The carrier could then be applied to one set of grids 180 degrees out of phase and the modulation, to the other set in parallel.

A brief check made on this scheme recently indicates that it is satisfactory. Two type 6L7 tubes with the carrier applied to No. 1 grids and the modulation applied to No. 3 grids produced the oscillogram of Fig. 3, Photograph R-334. This was made with 60 cycle square wave light variation and a 3240 cycle carrier. The balance was practically perfect.

3.8 - Miscellaneous Observations and Comments

One disadvantage in using the magnetic type multiplier as a facsimile scanner is that the unit as a whole is quite bulky due to the necessity of the magnetic field supply. The electrostatic type of multiplier which is being developed by the Electronic Research Laboratory at Camden will largely overcome this difficulty.

A small amount of dark current (from 5 to 10 microamps. at times) was observed in the particular tube tested. This increased several-fold when the ambient temperature of the tube compartment was allowed to rise 15 or 20 degrees centigrade above room temperature. This dark current is believed to be due largely to thermionic emission. Hence, if the tube is kept at normal room temperature the amount of dark current will be small compared to the normal output.

The output of the multiplier rises rapidly with the total applied voltage or rather, the voltage per stage. However, for a facsimile scanner head, flexible leads are usually necessary and space requirements are at a minimum so high voltage is undesirable. Consequently, if the 10 stage tube gives more than enough output to drive a suitable modulator then either the voltage per stage or the number of stages may be decreased.

4 - Summary of Results

4.1 - The maximum amount of light available at the photocell in a standard AA-914 scanner or one of similar type is in the order of 6.4×10^{-4} lumen.

4.2 - With this amount of light the dc output current of the 10 stage multiplier used in this investigation is in the order of 5×10^{-4} ampere for 130 volts per stage.

4.3 - With a light chopper frequency of 12,000 cycles per second the maximum load resistance that can be used without appreciable distortion of output waveform is 50,000 ohms.

4.4 - With 6.4×10^{-4} lumen of light (chopped) the peak value of voltage developed across the 50,000 ohm load is 25 volts.

4.5 - Additional stray or shunt capacitance in parallel with the load resistance alters the waveform as shown on Photograph R-333, Figs. 10, 12 and 14. If Fig. 12 is the case of maximum allowable distortion then the time constant (RC) of the load circuit should not exceed 5 microseconds. This same amount of distortion is also given by the curve of Fig. 2, sheet E which was computed from theoretical considerations.

4.6 - The theoretical development shows that in addition to the change in waveform caused by excessive stray capacitance there is also produced a lag in response. This lag in the voltage or current wave is almost equal to the time constant of the circuit.

4.7 - Excessive dark current results if the multiplier temperature is allowed to rise more than a few degrees centigrade.

4.8 - A carrier frequency can be successfully introduced into the multiplier by electrostatic means, but the resulting modulation contains a large dc component which cannot be removed without increasing the build up time.

5 - Conclusions

The electron multiplier should made a successful high speed facsimile scanner unit for the following reasons:

1. It has a large output of undistorted voltage (5×10^{-4} amp. through 50,000 ohms equals 25 volts) even with the small amount of light available in scanner systems.

2. Its frequency response is linear over the entire range covered by page-a-minute speed.

3. The electrostatic type of multiplier will not be too bulky to mount in a movable scanner head and requires no magnetic field structure.

4. Although twelve to fifteen hundred volts are needed this could be supplied by a rectifier and be properly insulated.

5. The output of the multiplier is sufficient to drive a modulator.

The electron multiplier and the associated equipment developed in this investigation are proving to be valuable laboratory tools for making circuit tests in connection with high speed facsimile requirements.

As a result of the work completed to date on this study, the circuit of Fig.1, sheet L, is suggested as the most promising scanner circuit in which an electron multiplier may be used. Although this circuit as a whole has not as yet been tried, all of the elements which comprise it have been found to be entirely satisfactory. The multiplier output (which is arranged to rise in plus polarity as the light increases) is applied to one set of grids of a balanced modulator unit. The carrier is applied on a second set of grids. A counter emf circuit is also proposed to improve the linearity of the modulator for low values of output. A final tube is used to combine the normal modulator output and the counter emf and give additional amplification.

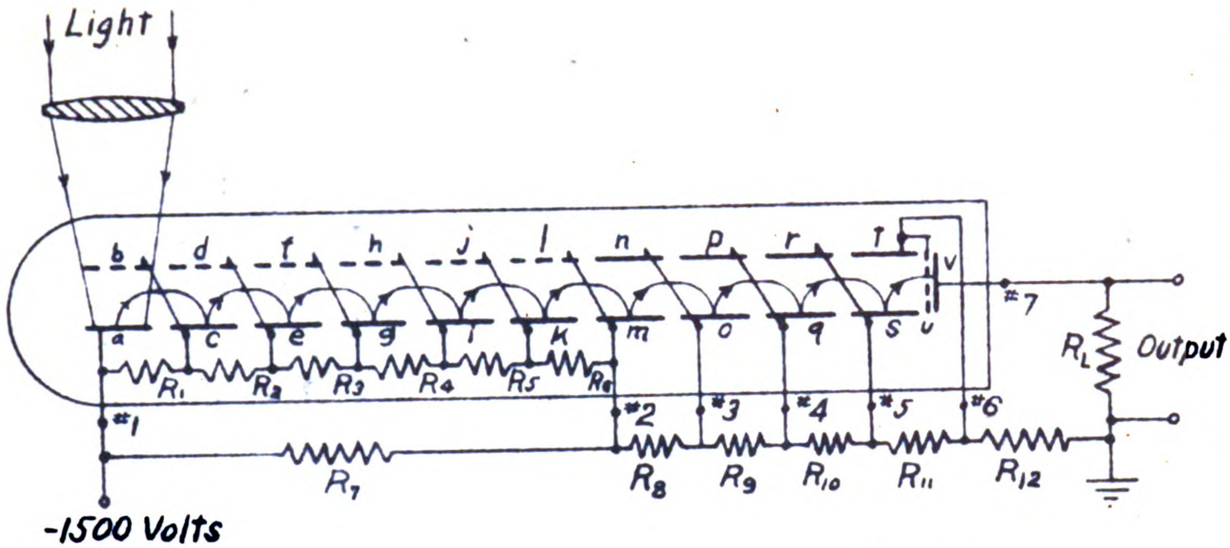

Fig. 1 10 Stage Electron Multiplier and Circuit.

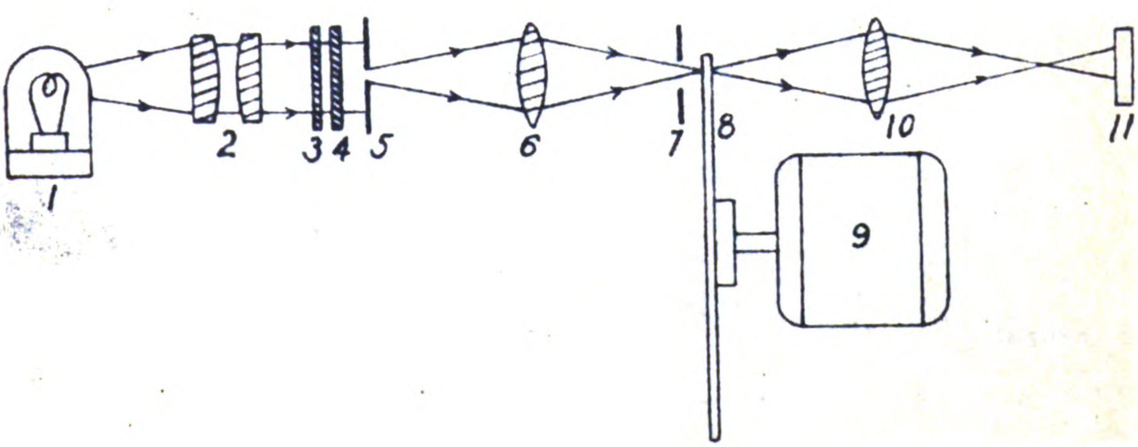

Fig. 2 Chopper Disc and Optical System.

ELECTRON MULTIPLIER AND ASSOCIATED EQUIPMENT

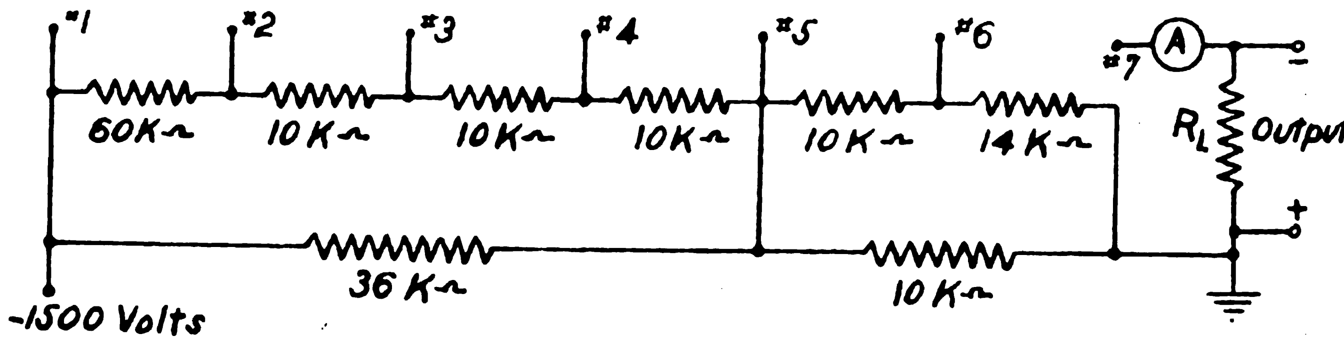

Fig. 1 Multiplier Circuit for Negative Output

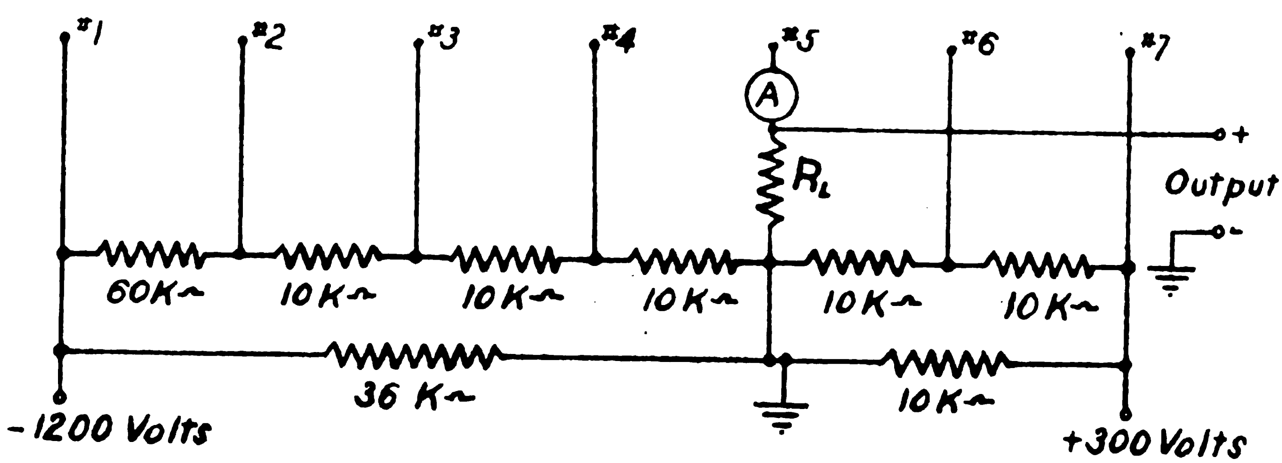

Fig. 2 Multiplier Circuit for Positive Output

ELECTRON MULTIPLIER CIRCUIT

SHEET C

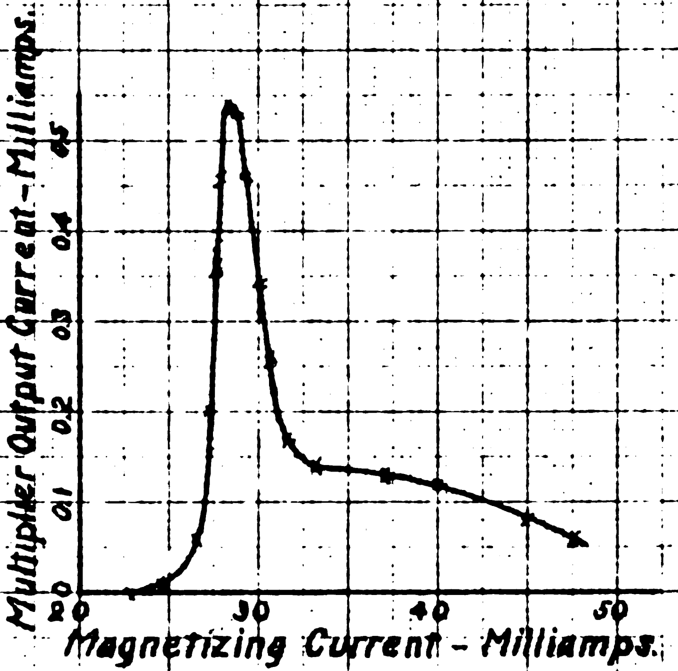

Fig. 1 RESONANCE CURVE

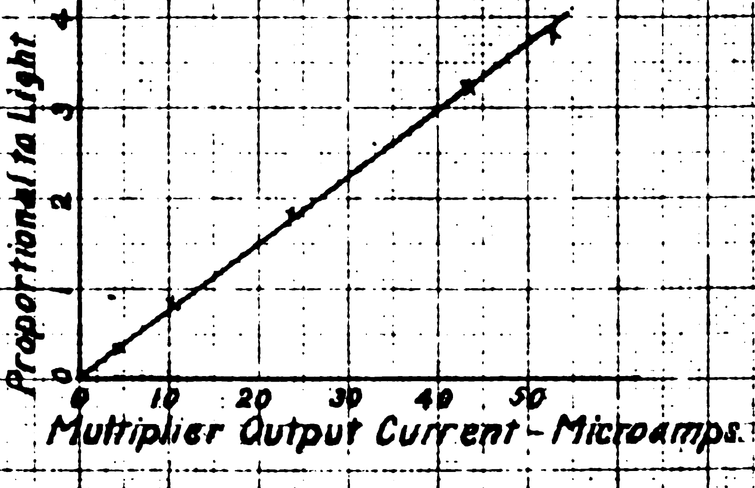

Fig. 2 LINEARITY CURVE

ELECTRON MULTIPLIER STATIC CHARACTERISTICS

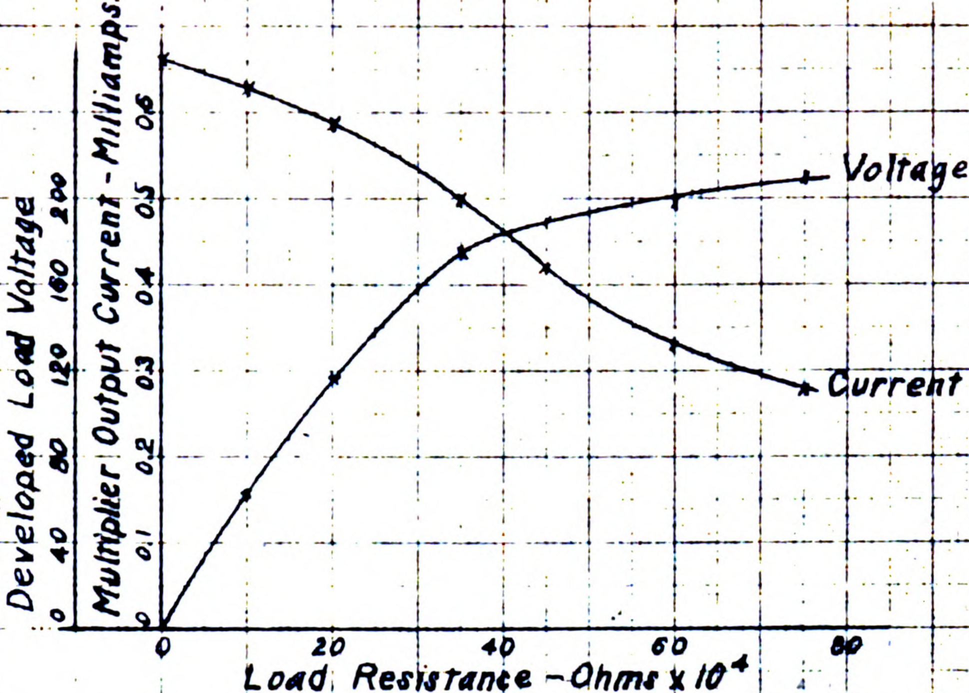

Fig. 1 LOAD RESISTANCE CURVES - Output Normal

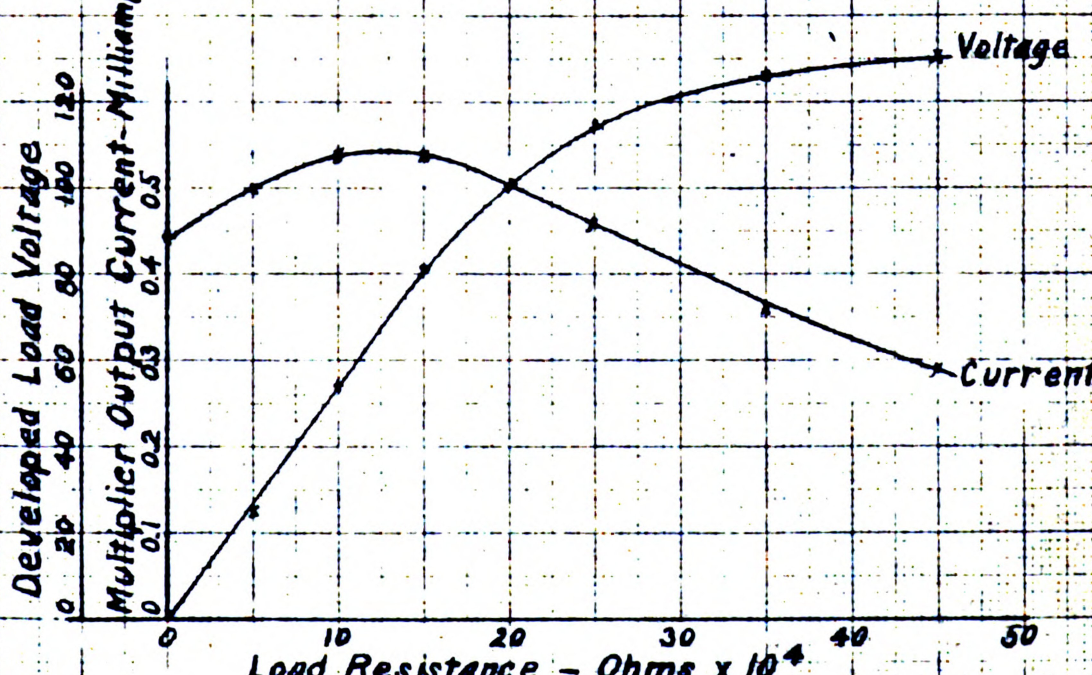

Fig. 2 LOAD RESISTANCE CURVES - Output Reversed in Polarity

ELECTRON MULTIPLIER STATIC CHARACTERISTICS

SHEET E

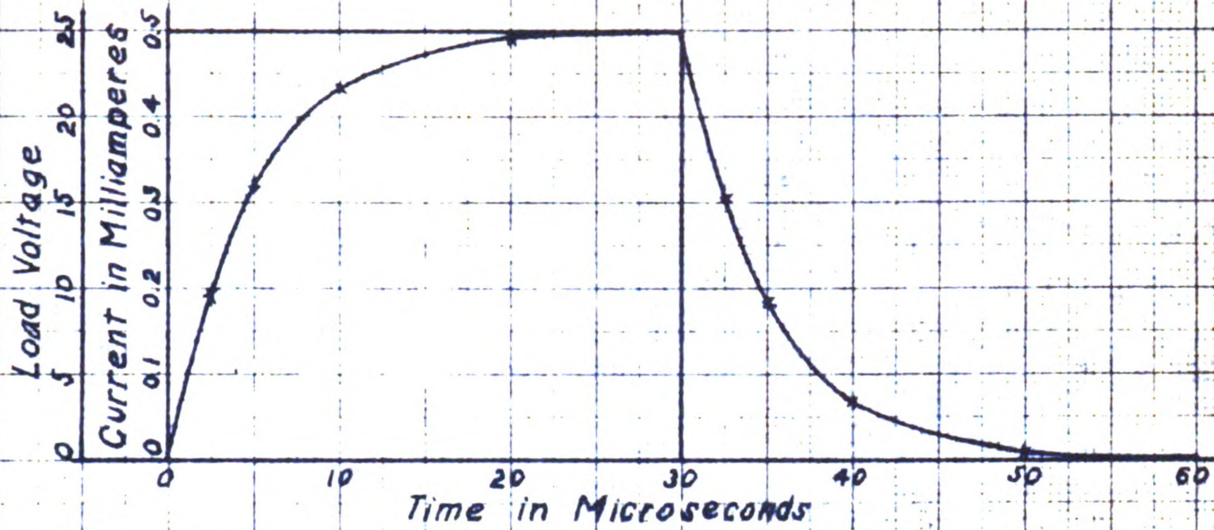

Fig. 1 SQUARE WAVE

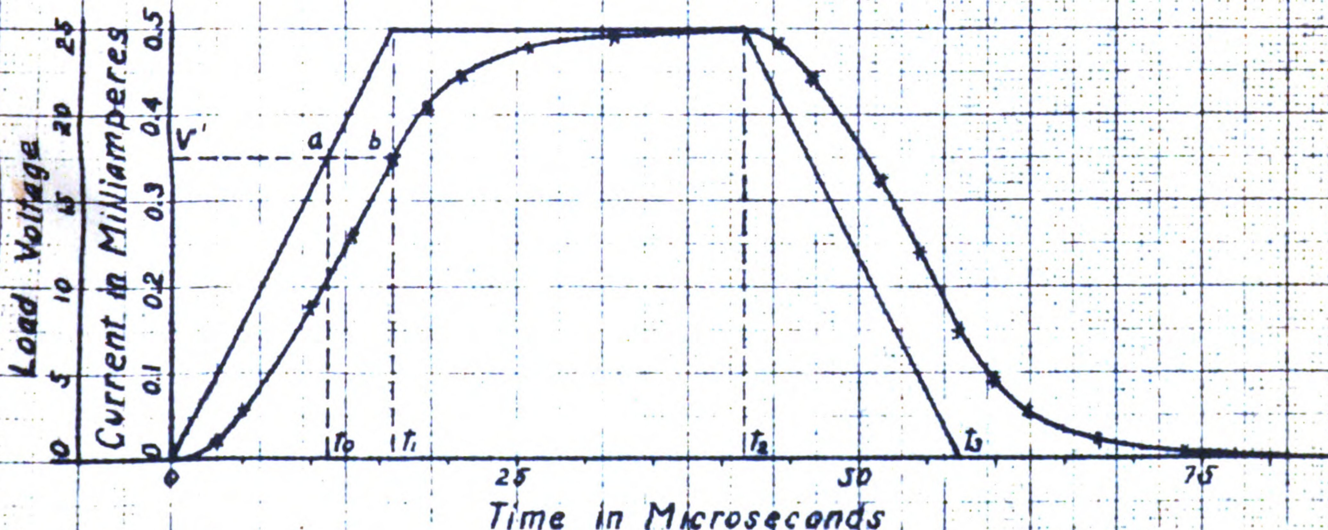

Fig. 2 TRAPEZOIDAL WAVE

ELECTRON MULTIPLIER LOAD CHARACTERISTICS

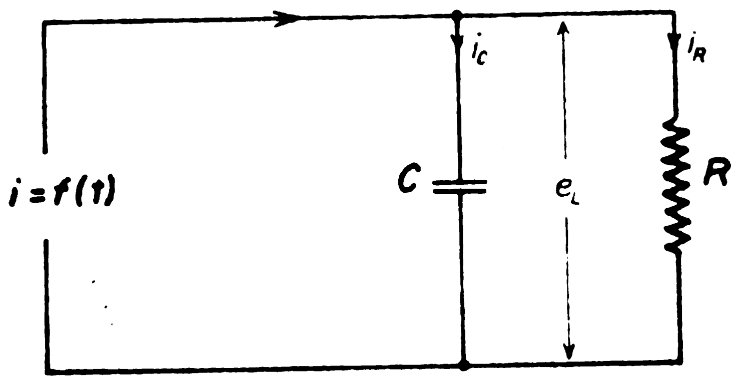

Fig. 1 Electron Multiplier Load Circuit

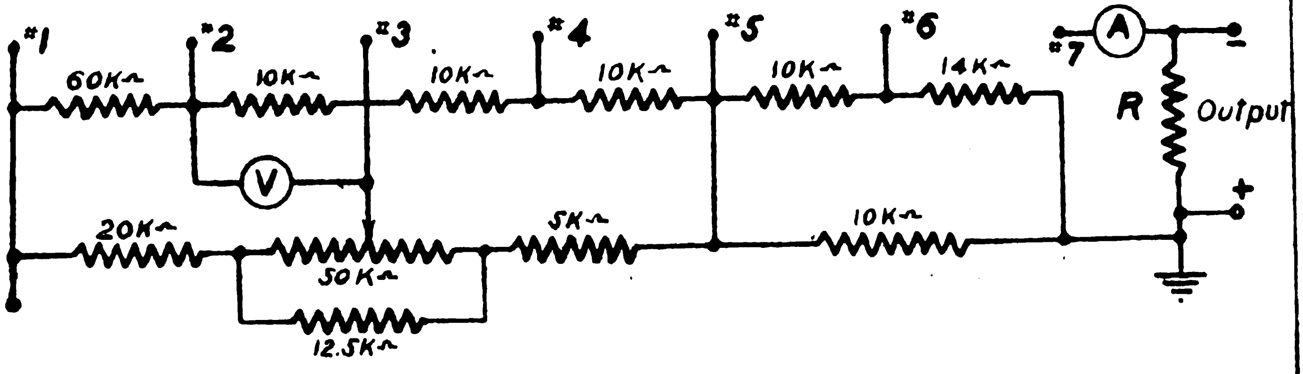

Fig. 2 Circuit for Obtaining Characteristic Shown on Sheet G

ELECTRON MULTIPLIER CIRCUITS

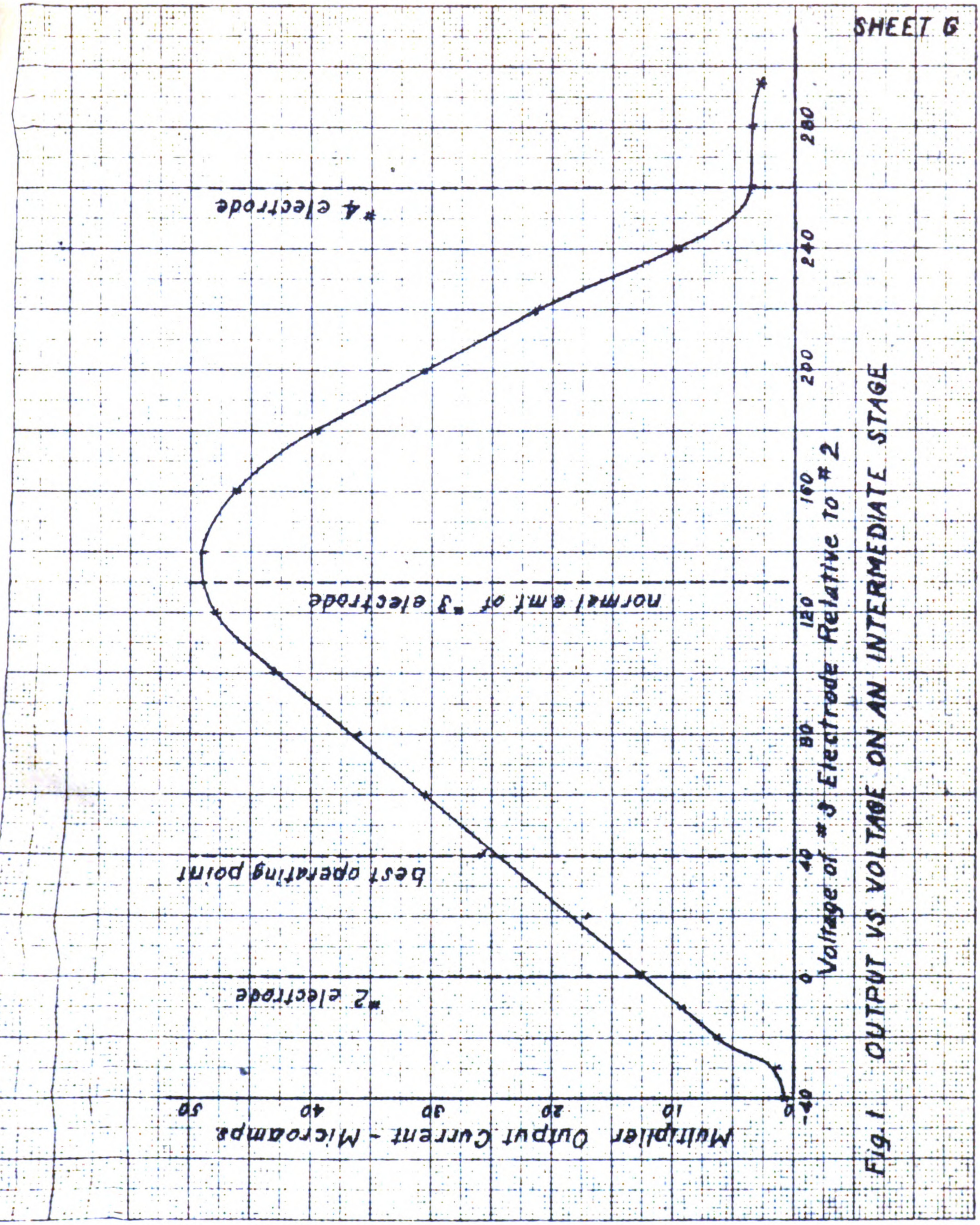

Fig. 1 OUTPUT VS. VOLTAGE ON AN INTERMEDIATE STAGE

ELECTRON MULTIPLIER
STATIC CHARACTERISTIC

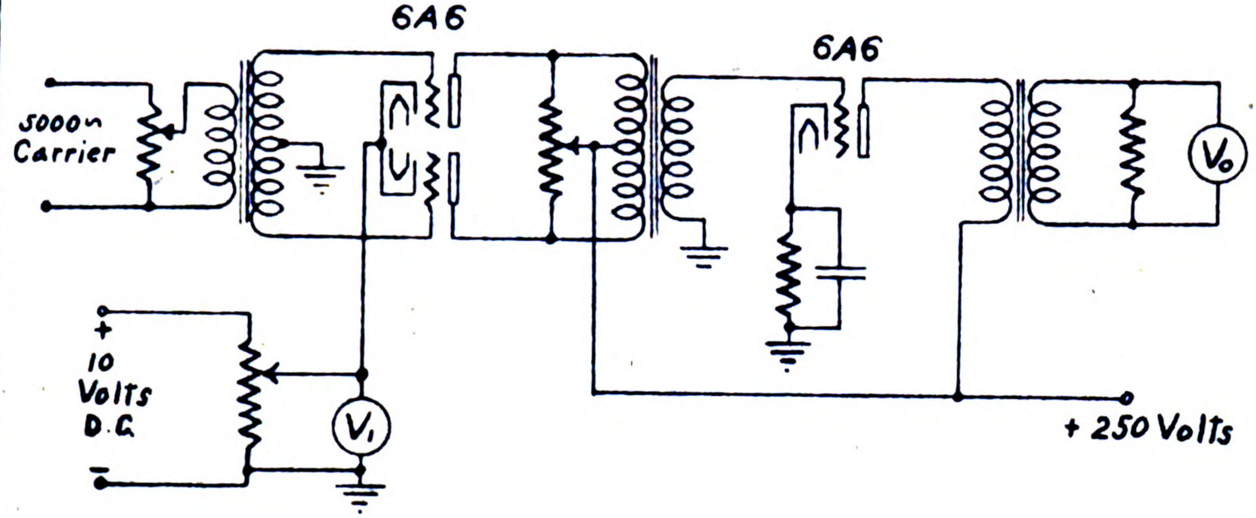

Fig. 1 Circuit for Determining Balanced Modulator Characteristic

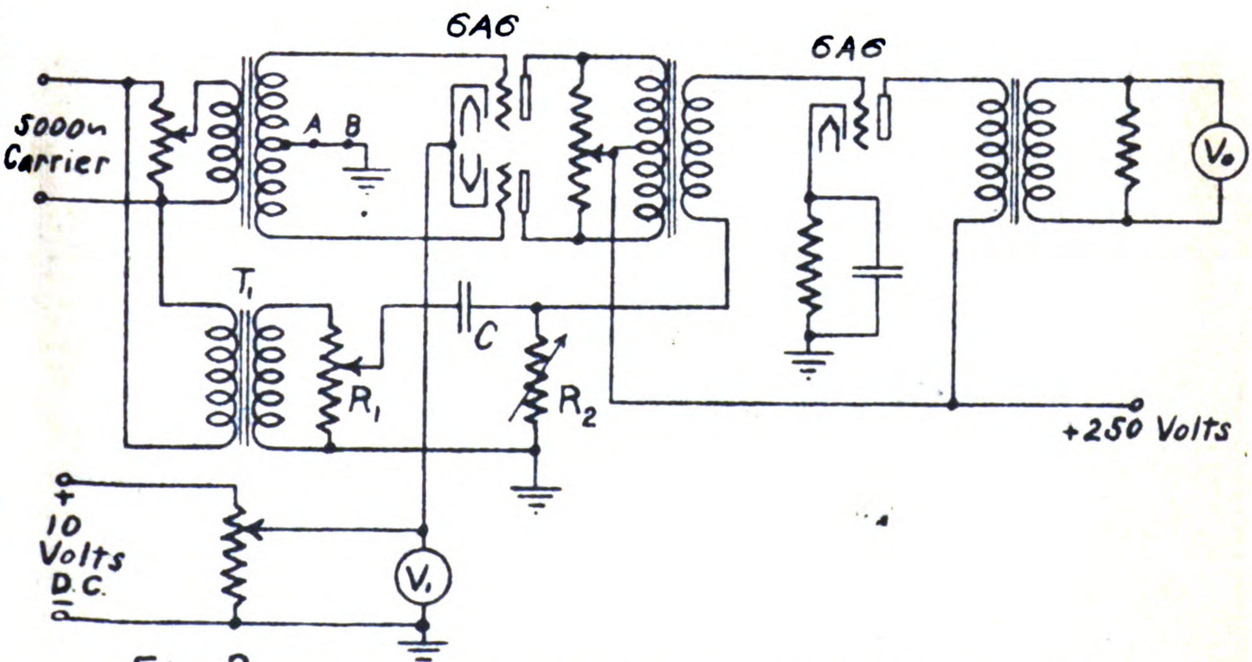

Fig. 2 Balanced Modulator with Counter E.m.f.

CIRCUITS FOR BALANCED MODULATOR CONSIDERATIONS

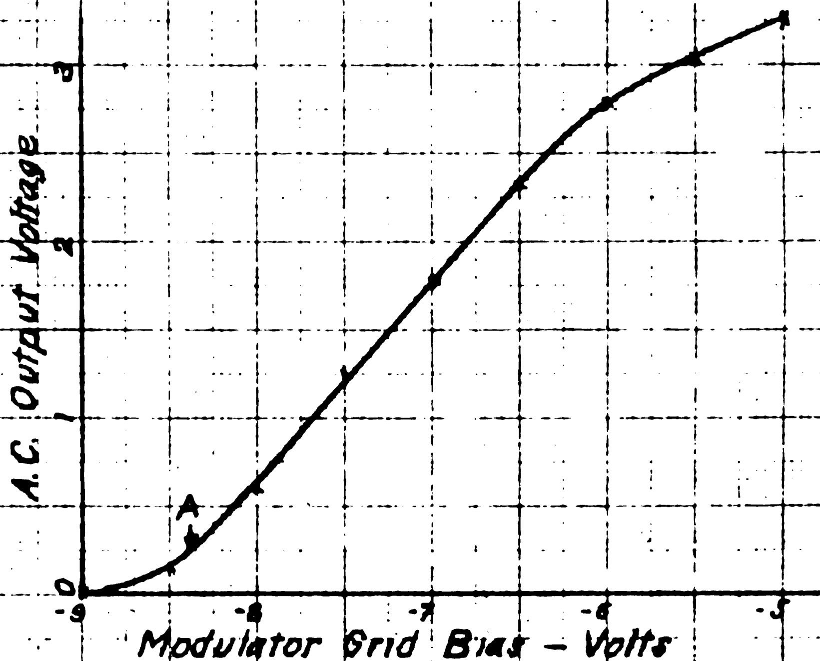

Fig. 1 NORMAL MODULATION CURVE

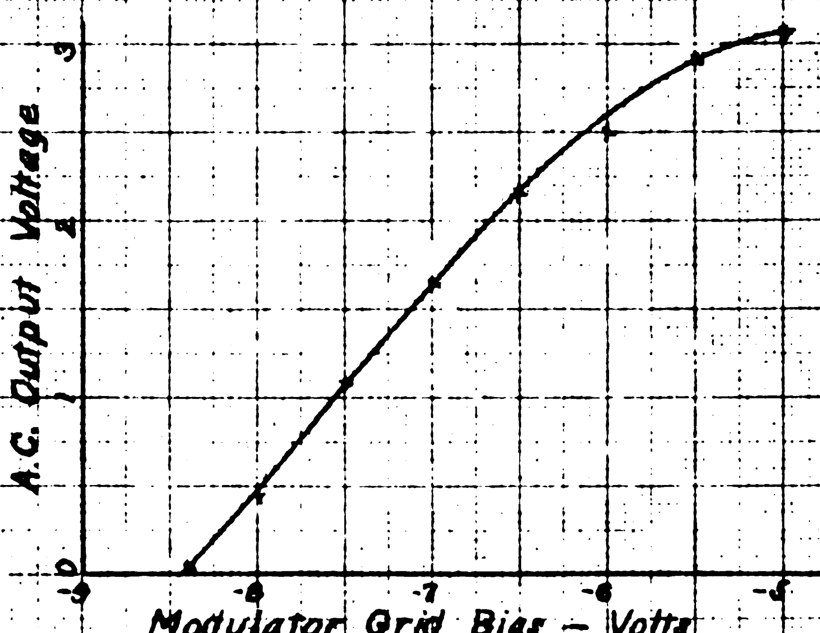

Fig. 2 COMPENSATED MODULATION CURVE

PUSH-PULL MODULATOR CHARACTERISTICS

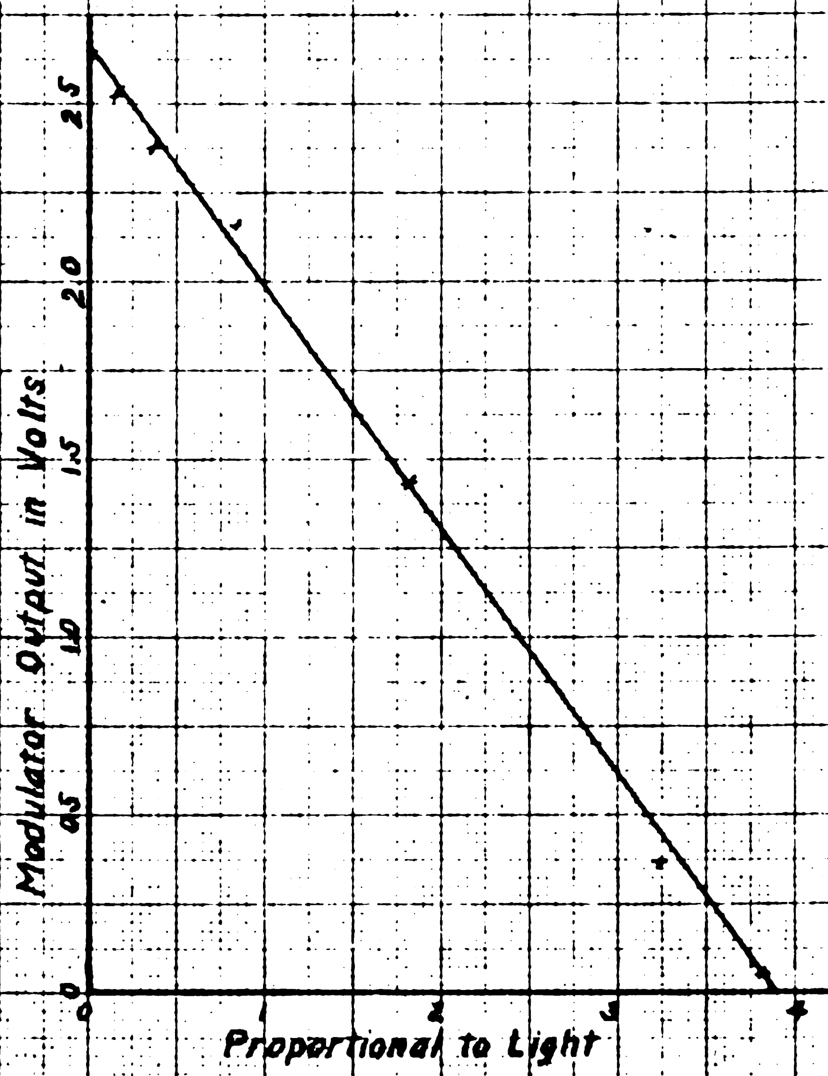

Fig. I OVERALL LINEARITY CURVE

ELECTRON MULTIPLIER AND
MODULATOR SYSTEM CHARACTERISTIC

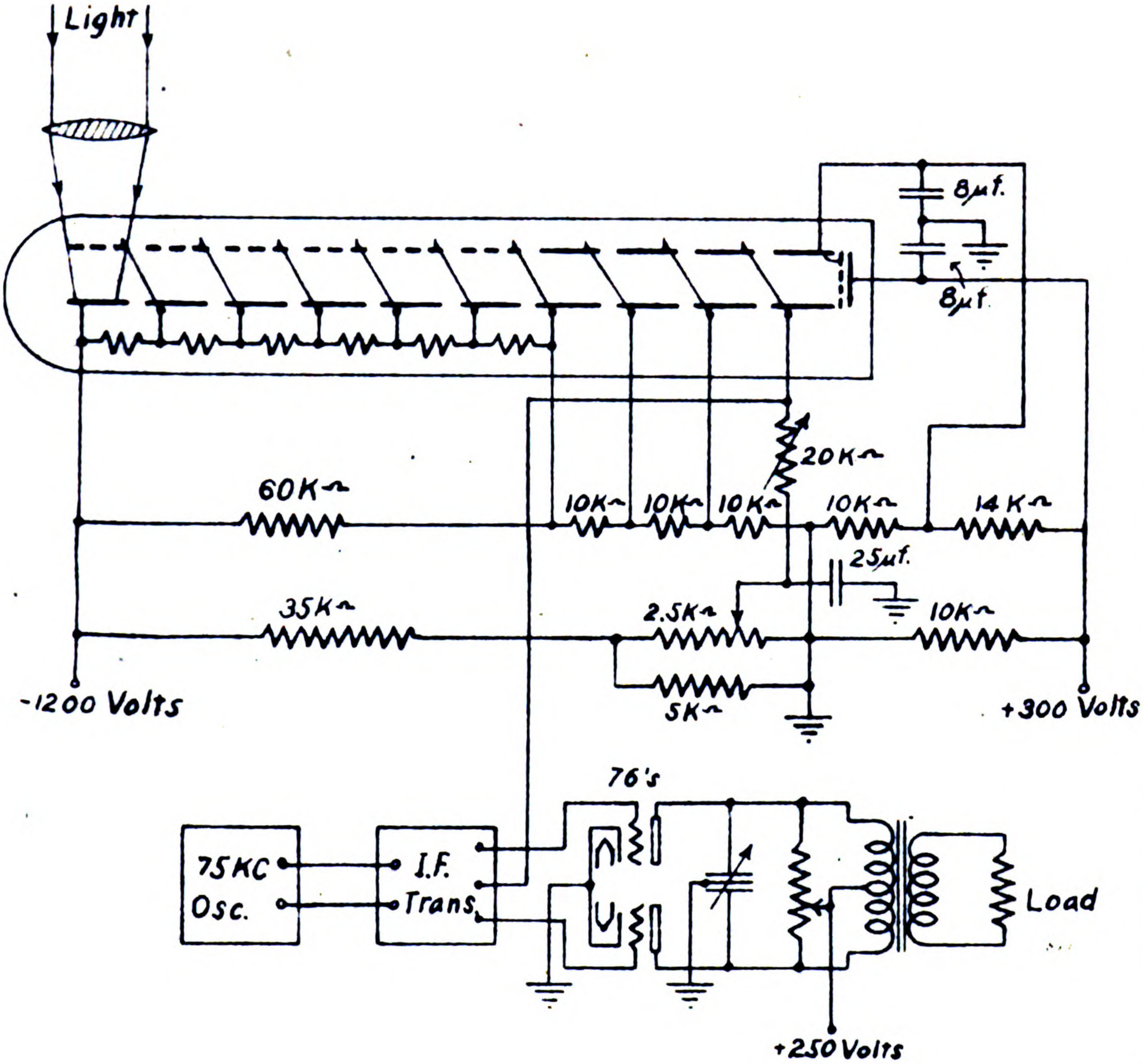

Fig. I ELECTRON MULTIPLIER DRIVING A BALANCED MODULATOR

ELECTRON MULTIPLIER CIRCUIT

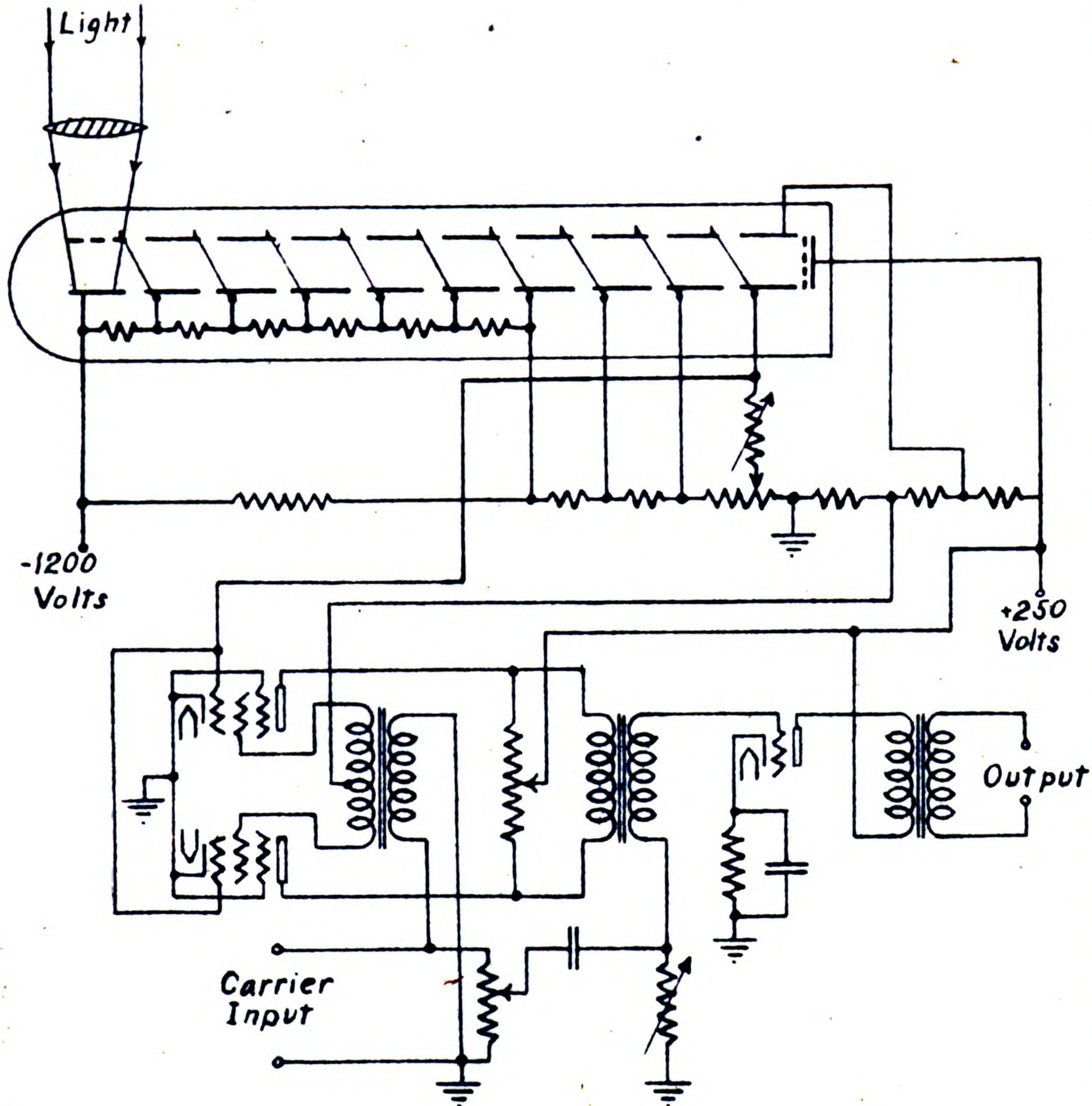

Fig. I Circuit for Proposed Electron Multiplier Scanner System

ELECTRON MULTIPLIER CIRCUIT

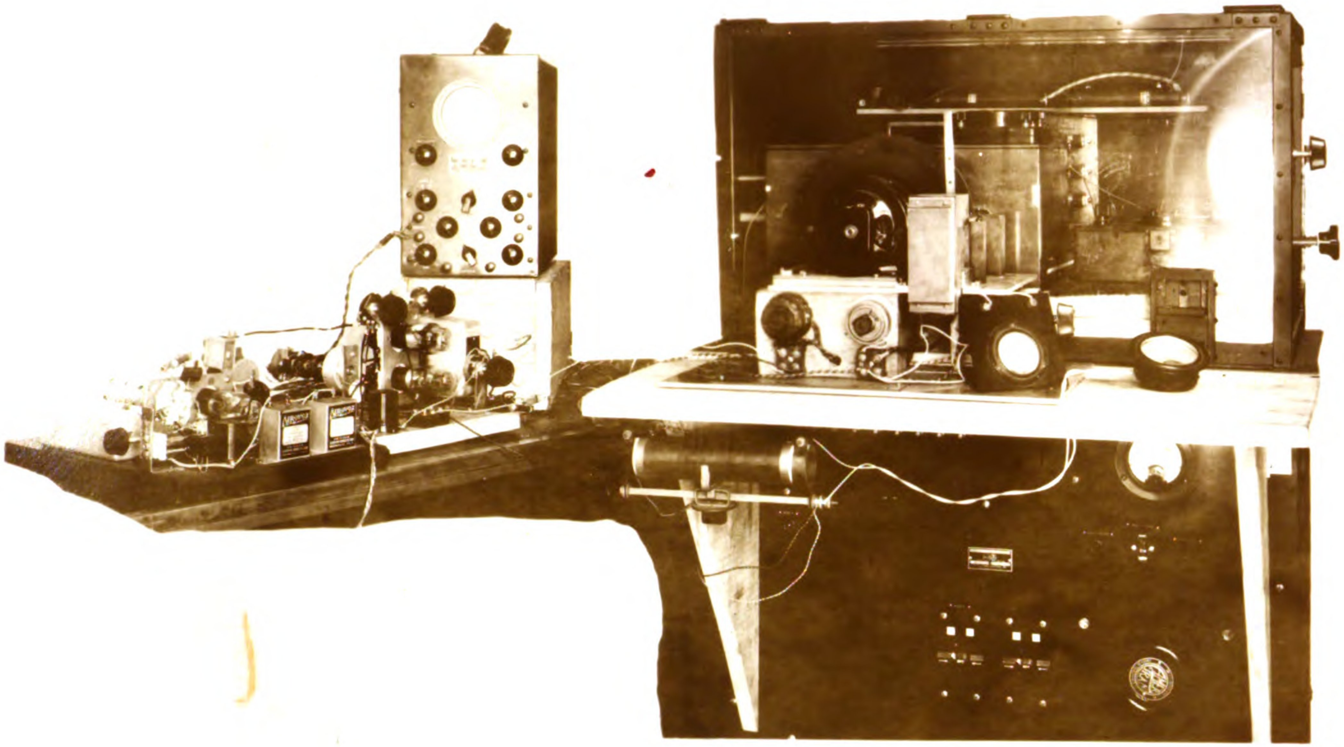

95230.

R-318

Fig. 1

Fig. 2

95229
R-31P

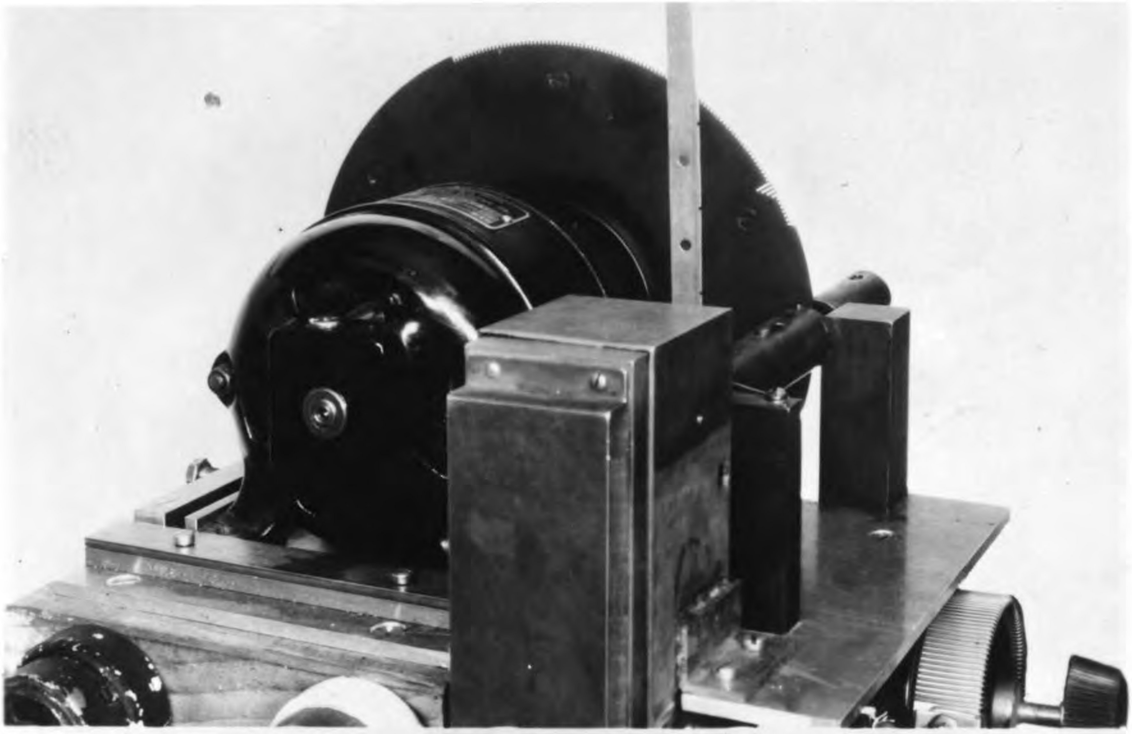

Fig. 1

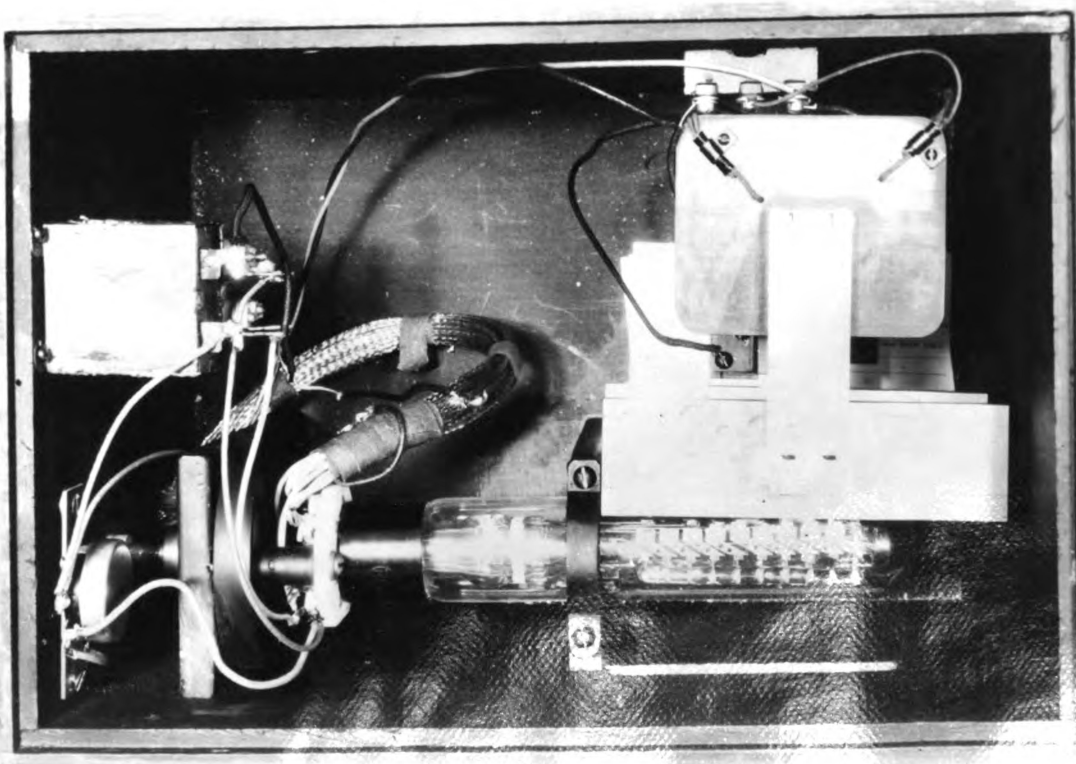

Fig. 2

95228.

Fig. 1 F = 8000 ~
R = 25000 Ω C = 0

Fig. 2 F = 12000 ~
R = 25000 Ω C = 0

Fig. 3 F = 8000 ~
R = 25000 Ω C = 0.0005 μf

Fig. 4 F = 12000 ~
R = 25000 Ω C = 0.0005 μf

Fig. 5 F = 8000 ~
R = 50000 Ω C = 0

Fig. 6 F = 12000 ~
R = 50000 Ω C = 0

Fig. 7 F = 60 ~
R = 50000 Ω C = 0

Fig. 8 F = 60 ~
R = 50000 Ω C = 0.005 μf

ELECTRON MULTIPLIER OUTPUT WAVEFORMS

95227
R-332

Fig. 9 R = 100,000 ~
C = 0

Fig. 10 R = 100,000 ~
C = 0.0001 μf.

Fig. 11 R = 50,000 ~
C = 0

Fig. 12 R = 50,000 ~
C = 0.0001 μf.

Fig. 13 R = 25,000 ~
C = 0

Fig. 14 R = 50,000 ~
C = 0.0002 μf.

Fig. 15 R = 100,000 ~ C = 0
Light Reduced

Fig. 16 R = 16,000 ~ C = 0
Light Increased

ELECTRON MULTIPLIER OUTPUT WAVEFORMS

95226.

R-333

ELECTRON MULTIPLIER MODULATED WAVEFORMS

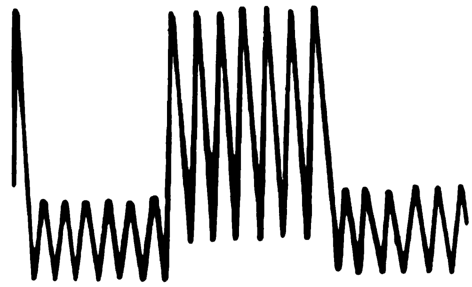

Fig. 1 60~ Chopper
810~ Carrier

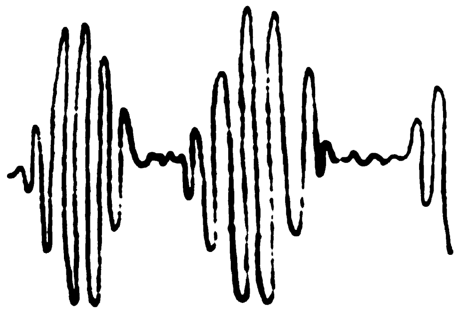

Fig. 2 12,000~ Chopper
75 KC. Carrier

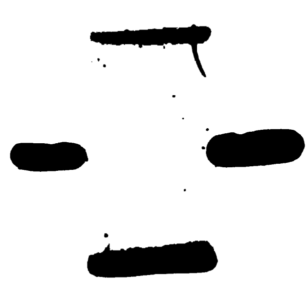

Fig. 3 60~ Chopper
3240~ Carrier

95225.
R-334


95214- R-344